

Adapted Spectral Clustering for Evaluation and Classification of DCE-MRI Breast Tumors

Sylvia Glaßer¹, Sophie Roscher¹, Bernhard Preim¹

¹Department for Simulation and Graphics, OvG-University Magdeburg
glasser@isg.cs.uni-magdeburg.de

Abstract. Classification of breast tumors in perfusion DCE-MRI solely based on dynamic contrast enhanced magnetic resonance data is a challenge. Many studies employ grouping of voxels into regions via clustering for further analysis. However, the clustering result strongly depends on the chosen clustering algorithm and its parameter settings. In this paper, we explain how spectral clustering can be adapted to breast tumor data and suggest how the clustering parameters can be automatically derived such that no pre-defined user input, e.g., cluster number, is necessary. The presented spectral clustering approach has the great advantage of generating spatially connected regions. Furthermore, it can be enabled for automatic classification and yields similar results as previous approaches.

1 Introduction

For the evaluation of breast tumors, conventional X-ray mammography is in some cases not sufficient or not diagnostically relevant, in particular in younger woman where the dense breast tissue does not reveal pathologic masses. To confirm the malignancy or benignity of such unclear lesions as well as to detect small metastasis in case of a known primary tumor, dynamic contrast enhanced magnetic resonance imaging (DCE-MRI) is applied. DCE-MRI has a high sensitivity when compared to X-ray, however, the specificity is only moderate. Thus, in clinical research, the automatic classification of breast lesions based on their DCE-MRI-based contrast enhancement and morphology is an active research area [1]. In clinical practice, the radiologist defines a region of interest (ROI) in the most suspect part of the tumor and analyzes the average relative contrast enhancement (RE) over time of this ROI. Based on washin and washout characteristics from the RE curve as well as analysis of the tumor's morphology, the radiologist carries out a diagnosis. The manual ROI placement suffers from intra- and inter-observer variability which can strongly hamper the diagnostic result since a tumor is as malignant as its most malignant part. Furthermore, when a ROI covers benign and malignant tumor tissue, the ROI's average RE curve may be not appropriate to assess the tumor's malignancy. In spite of these shortcomings, determination of the most suspect ROI and thus the most suspect tumor part is important for further diagnosis like core needle biopsy. To solve these problems, we introduce a spectral clustering approach to group voxels

into homogeneous regions and to maintain spatial connectivity of these regions. Then, the most suspect ROI can be identified and employed for automatic tumor classification.

Our approach is based on our previous work [2], where density-based clustering is employed to breast DCE-MRI lesions. Then, a most suspect region is extracted that serves as ROI for further analysis. Similarly, region merging is employed to group and identify suspect regions of DCE-MRI tumors in [3]. The results were employed for automatic breast tumor classification based on tumor heterogeneity by Preim et al. [4], yielding an increased heterogeneity for malignant tumors. However, the spatial connectivity of the resulting regions can be improved by our approach and we achieve similar or even better classification results. Also related to our work is the study of Chen et al. [5]. They apply fuzzy c -means clustering and extract the most characteristic RE curve for breast tumor classification but they can not automatically determine a most suspect ROI.

2 Material and Methods

2.1 Tumor Data

We tested our approach with a database consisting of 68 breast lesions from DCE-MRI data. From the 68 lesions, 31 tumors are classified as benign lesions and 37 as malignant lesions. The classification of the lesions was confirmed by histopathology (60 cases) or follow-up examination after 6 - 9 months (8 cases). The database only contains tumors that have been detected in MRI and that cannot be detected in conventional x-Ray mammography. The identification and delineation of the lesion from background was conducted by an experienced radiologist. The MR image parameters include an in-plane resolution of $\approx 0.67 \times 0.67 \text{mm}^2$ with an image matrix of $\approx 528 \times 528$, ≈ 100 slices with a slice gap of 1.5mm acquired at five or six time steps, i.e. one pre-contrast and four to five post-contrast images. MRI perfusion data sets suffer from motion artifacts due to breathing and patient's movement. Thus, an elastic registration was carried out for motion correction [6]. The signal intensities values SI_t of the data sets at time step t were normalized with the pre-contrast signal intensity SI_0 to extract relative enhancement RE_t values; $RE_t = (SI_t - SI_0)/SI_0 \times 100$. For each voxel, the following descriptive perfusion parameters were extracted:

- Max_{RE} , the maximum of the RE values
- T_{Max} , the point in time when RE_t equals Max_{RE} ,
- washin , the value of RE_2 , where $t = 2$ is the first time step after the early post-contrast phase,
- washout , the normalized difference between the last time step $t = n$ and $t = 2$, i.e. $(RE_n - RE_2)/(n - 2)$.

For further characterization, we assign each voxel's RE curve to an 3TP class, based on the three-time-point (3TP) method [7]. The 3TP method defines three

types of initial RE enhancement (slow, intermediate and fast) and three types of curve shapes (washin, plateau, washout) yielding 9 classes (see Fig. 1). It involves three well chosen time steps: t_a , the first point in time before the contrast agent injection, t_b , 2 min after t_a and t_c , 4 min after t_a . Since our study contains five to six time steps due to different scanning parameters, we assign the third time t_3 step to t_b and the last time step t_n to t_c . The selection of parameters and the adaption of the 3TP method is based on our previous work [2].

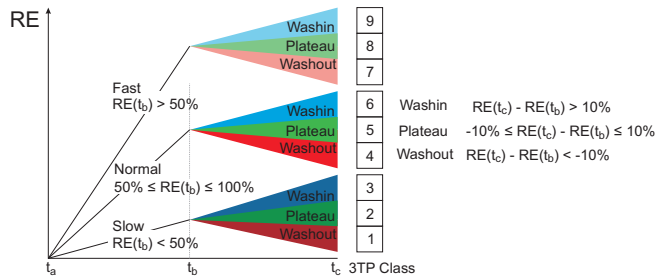


Fig. 1. The nine classes according to the 3TP method [7].

2.2 Methods

Our approach consists of two steps: the adoption of spectral clustering for each tumor and the feature extraction on which the classifier will be learned.

Step 1: Clustering in the Spectral Space. We apply a spectral clustering method to divide each tumor into homogeneous and spatially continuous clusters based on the normalized (via z-scoring) perfusion parameters Max_{RE} , T_{Max} , washin, and washout.

Spectral clustering employs graph cuts such that edges between different groups (i.e., clusters) have very low weights and edges within the same cluster have high weights. Such a graph cut can be easily found by using the eigenvectors and eigenvalues of a specific matrix - the *Laplacian matrix* - to map the original data points to a low dimensional space [8]. In this new representation, clusters can be easier separated (regarding the high-dimensional space) by applying simple clustering techniques like k -means. A weighted, undirected graph is constructed from the initial data set. Each node represents a data point and each edge the similarity between two points with a symmetric and non-negative similarity function. Based on this affinity matrix, a Laplacian matrix is constructed and an eigenvalue decomposition is performed. The eigenvalues and eigenvectors are used to map the original data points to the k dimensional vectors of the spectral domain. For a more detailed review, we refer to [8].

We use the Ng-Jordan-Weiss Algorithm (see also [8]) to directly partition the data into k groups. The similarity graph is constructed based on the descriptive perfusion parameters. Each node of the graph represents a voxel of the corresponding breast tumor. Hence, the tumor data are represented in an regular

orthogonal 3D grid and each node is connected to its adjacent nodes within a 26-neighborhood. We use the Gaussian similarity function [8]:

$$s(x_i, x_j) = \exp\left(-\frac{\text{dist}(x_i, x_j)}{2\sigma^2}\right)$$

to represent the local neighborhood relationships. The distance $d(x_i, x_j)$ between two points is measured by using the cosine similarity of the corresponding perfusion parameter values [8]. The scaling parameter σ describes how rapidly the affinity decreases with the distance between x_i and x_j . Instead of manually selecting σ , we use the approach described in [9] to calculate a local scaling parameter for each data point. Although we still have to select the n number of neighbors that should be considered to compute this scale, this selection is independent of scale [9]. We applied three internal cluster validation measurements [10]: the Davies-Bouldin index, the Dunn index, and the Calinski-Harabasz index to empirically find an n that provides the best clustering result. We varied n in the range of [3..11] and analyzed the corresponding validation indices yielding the best result for $n = 3$. In spectral clustering, we also have to specify the number of clusters k . For the presented method, the three validation indices are applied again. Then, the best k is chosen via majority voting based on the values of the validation indices. If no majority exists, we employ the Davies-Bouldin index. For each data set, the spectral clustering is computed several times with different clusters k ($k = \{3..9\}$) and the optimal k is selected according to the validation indices. In summary, the distance function $d(x_i, x_j)$ detects similar descriptive perfusion parameter values and the 26-neighborhood yields the spatial connectivity of voxels in a cluster. This is an advantage in comparison to the density-based clustering approach presented in [2].

Step 2: Feature Extraction for Classification. Based on the spectral clustering result, we extract features to compare the discriminative power of our clustering result. Based on our previous work [2], we choose one cluster as most suspect region. Therefore, we analyze the 3TP class of the clusters averaged RE curve and again employ the 3TP class ranking: 7, 9, 8, 4, 6, 5, 1, 3, 2. Thus, if three clusters exist, with average curves of 3TP classes 7, 4 and 8, we choose the cluster with average RE curve classified as 3TP class 7.

We employ the following features for each tumor to learn a classifier:

- biological features, i.e., age and tumor size in mm^3 ,
- features of the chosen cluster and its average RE curve, i.e., washin, washout, and 3TP class, as well as the percentage cluster size (when compared to the whole tumor), and
- features characterizing the whole tumor clustering result, i.e. the number of clusters, the separability (i.e., the inter-cluster variance), the homogeneity (i.e. the averaged intra-cluster variance), and the similarity measures Purity, Jaccard index and F1 score based on the comparison of the clustering result and the 3TP method classification of all tumor voxels.

The classifier was created with the Weka library, a Java software library that encompasses algorithms for data analysis and predictive modeling [11]. Based on our previous work [2], a decision tree was trained with the C4.5 classification algorithm [12]. It automatically selects features with high discriminative power. It performs 10-fold cross validation and requires at least two instances (two tumors) for each tree leaf. The best tree result is depicted in Figure 2.

3 Results

For the automatic classification of our database, we learned the decision tree, depicted in Figure 2. It correctly classifies 56 of 68 tumors, i.e. 82.24%. Inherent to decision trees, the most important features are at top levels, i.e., closer to the root, since the splitting a larger set of tumors. Hence, the feature *patient age* was employed as most important feature, however all other attributes characterize the tumor’s heterogeneity and kinetic contrast enhancement behavior. Due to the specialty of our database (only suspicious or malignant lesions but no typical benign ones were included), we do not consider specificity or sensitivity, but the number of correctly classified tumors. The results are similar to our previous work [2], but we do only employ 10-fold cross validation instead of 5 folds. However, the benefit is the improved identification of the most suspect ROI w.r.t. the spatial connectivity, see Figure 3. Hence, no outliers are produced. Nevertheless, the identified most suspect cluster has similar discriminating power when applied for automatic classification as previous results [2].

4 Discussion

In this paper, we explained how spectral clustering can be successfully adapted to breast DCE-MRI tumors. We carried out k -means in the spectral domain and provide automatic parameter choices for the input parameters. The clustering result produces spatially connected homogeneous regions as well as a most suspect ROI, and achieves similar classification results as proposed in literature.

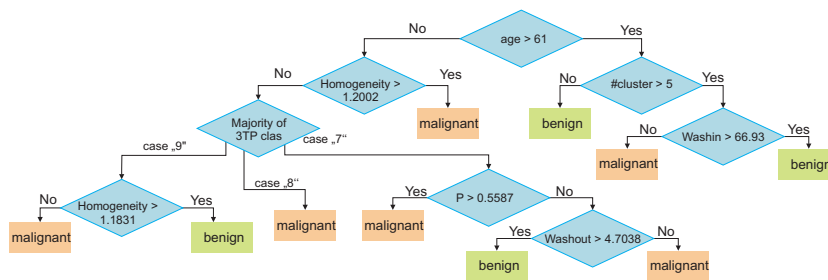
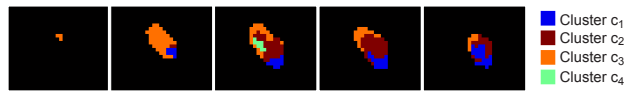


Fig. 2. Learned decision tree: the attributes at the upper part of the tree are the most important ones.

Fig. 3. Five slices showing the clustering result for a small breast tumor.

Our results are in particular promising, since the employed database comprises only tumors that are very hard to differentiate into benign and malignant ones. Hence, only histopathologic evaluation or follow-up could confirm the diagnosis. For future work, a bigger study, 5-fold cross validation and the combination with morphologic features should be carried out. *Acknowledgments.* We thank Myra Spiliopoulou and Uli Niemann for fruitful discussions. This work was supported by the DFG project SPP 1335 "Scalable Visual Analytics".

References

1. Schnall MD, Blume J, Bluemke DA, et al. Diagnostic Architectural and Dynamic Features at Breast MR Imaging: Multicenter Study. *Radiology*. 2006;238(1):42–53.
2. Glaßer S, Niemann U, Preim B, Spiliopoulou M. Can we Distinguish Between Benign and Malignant Breast Tumors in DCE-MRI by Studying a Tumors Most Suspect Region Only? In: *Proc. of Symposium on Computer-Based Medical Systems*; 2013. p. 59–64.
3. Glaßer S, Preim U, Tönnies K, et al. A Visual Analytics Approach to Diagnosis of Breast DCE-MRI Data. *Computers and Graphics*. 2010;34(5):602 – 611.
4. Preim U, Glaßer S, Preim B, et al. Computer-Aided Diagnosis in Breast DCE-MRI – Quantification of the Heterogeneity of Breast Lesions. *European Journal of Radiology*. 2012;81(7):1532 – 1538.
5. Chen W, Giger ML, Bick U, et al. Automatic Identification and Classification of Characteristic Kinetic Curves of Breast Lesions on DCE-MRI. *Medical Physics*. 2006;33(8):2878–87.
6. Rueckert D, Sonoda L, Hayes C, et al. Nonrigid Registration Using Free-Form Deformations: Application to Breast MR Images. *IEEE Trans Med Imaging*. 1999;18(8):712–21.
7. Degani H, Gusic V, Weinstein D, et al. Mapping pathophysiological features of breast tumors by MRI at high spatial resolution. *Nat Med*. 1997;3:780–782.
8. Von Luxburg U. A Tutorial on Spectral Clustering. *Statistics and computing*. 2007;17(4):395–416.
9. Zelnik-Manor L, Perona P. Self-Tuning Spectral Clustering. In: *Advances in neural information processing systems*; 2004. p. 1601–1608.
10. Rendon E, Abundez I, Arizmendi A, Quiroz E. Internal versus External Cluster Validation Indexes. *International Journal of Computers and Communications*. 2011;5(1):27 – 34.
11. Holmes G, Donkin A, Witten IH. WEKA: a machine learning workbench. In: *Proc. of Conf. on Intelligent Information Systems*; 1994. p. 357 –361.
12. Quinlan JR. *C4.5: Programs for Machine Learning*. Morgan Kaufmann Publishers; 1993.